



# Journal of Chemistry and Technologies

pISSN 2663-2934 (Print), ISSN 2663-2942 (Online).

journal homepage: <http://chemistry.dnu.dp.ua>  
editorial e-mail: [chem.dnu@gmail.com](mailto:chem.dnu@gmail.com)



UDC 662.756:620.92:66.095.26

## PVA-CoFe<sub>2</sub>O<sub>4</sub>-BIOCHAR COMPOSITES: STRUCTURE AND PROPERTIES

Liliya A. Frolova<sup>1</sup>, Dmytro Yu. Saltykov<sup>2</sup>, Oleksandr I. Kushnerov<sup>2</sup>, Kostyantyn V. Olkhov<sup>1</sup>,  
Maksim O. Nikitin<sup>1</sup>, Dmytro O. Rodin<sup>1</sup>

<sup>1</sup>Ukrainian State University of Science and Technologies, 8 Nauky Ave., Dnipro, 49005, Ukraine

<sup>2</sup>Oles Honchar Dnipro National University, 72 Nauky Ave., Dnipro, 49010, Ukraine

Received 25 July 2025; accepted 10 September 2025; available online 25 December 2025

### Abstract

PVA-CoFe<sub>2</sub>O<sub>4</sub>-biochar composites were synthesized by a two-stage combined method. The resulting composites were characterized by X-ray diffraction, scanning electron microscopy, UV-visible absorption spectroscopy, vibrational magnetometry, and vector microwave analysis. The results of electron microscopy show that biochar has a block structure with large pores, so this structure can be used in the creation of composites. The magnetic properties depend on the content of cobalt ferrite in the composite. The results of the study of photocatalytic properties showed that the rate of destruction of methylene blue (MB) is 50–98% after 60 min of UV radiation. It was established that the reaction of photocatalytic decomposition of MB obeys pseudo-first-order kinetics. Among these catalysts, biochar showed the highest rate constant of 0.085 min<sup>-1</sup>, PVA/CoFe<sub>2</sub>O<sub>4</sub>-biochar composites – 0.05 min<sup>-1</sup>.

When studying the absorption of electromagnetic radiation in the radar range from 8 GHz to 12 GHz by PVA/CoFe<sub>2</sub>O<sub>4</sub>-biochar composites, it was found that with an increase in the ratio of CoFe<sub>2</sub>O<sub>4</sub>-biochar components to 0.67 wt. parts CoFe<sub>2</sub>O<sub>4</sub>, the absorption losses of the composite reach –14.15 dB/mm at a frequency of 8 GHz and –12.37 dB at a frequency of 12 GHz.

**Keywords:** magnetic properties; spinel; X-ray phase analysis.

## КОМПОЗИТИ PVA-CoFe<sub>2</sub>O<sub>4</sub>-БІОЧАР: СТРУКТУРА ТА ВЛАСТИВОСТІ

Лілія А. Фролова<sup>1</sup>, Дмитро Ю. Салтиков<sup>2</sup>, Олександр І. Кушнеров<sup>2</sup>, Костянтин В. Ольхов<sup>1</sup>,  
Максим О. Нікітін<sup>1</sup>, Дмитро О. Родін<sup>1</sup>

<sup>1</sup>Український державний університет науки і технологій, , просп. Науки, 8, Дніпро, 49005, Україна

<sup>2</sup>Дніпровський національний університет імені Олеся Гончара, просп. Науки, 72, Дніпро, 49010, Україна

### Анотація

Композити ПВС-CoFe<sub>2</sub>O<sub>4</sub>-біовугілля синтезовані двостадійним комбінованим методом. Отримані композити були охарактеризовані методами рентгенівської дифракції, скануючої електронної мікроскопії, спектроскопії поглинання в УФ-видимій області, вібраційної магнітометрії та векторного мікрохвильового аналізу. Результати електронної мікроскопії показують, що біовугілля має блокову структуру з великими порами, тому ця структура може бути використана у створенні композитів. Магнітні властивості залежать від вмісту фериту кобальту в композиті. Результати дослідження фотокаталітичних властивостей показали, що швидкість деградації метиленового синього (МС) становить 50–98 % після 60 хв дії УФ-випромінювання. Встановлено, що реакція фотокаталітичного розкладу МВ підпорядковується кінетиці псевдопершого порядку. Серед цих каталізаторів біовугілля показало найвищу константу швидкості 0,085 хв<sup>-1</sup>, композити PVA/CoFe<sub>2</sub>O<sub>4</sub>-біовугілля – 0,05 хв<sup>-1</sup>. Під час вивчення поглинання електромагнітного випромінювання в радіолокаційному діапазоні від 8 ГГц до 12 ГГц композитами PVA/CoFe<sub>2</sub>O<sub>4</sub>-біовугілля встановлено, що зі збільшенням співвідношення компонентів CoFe<sub>2</sub>O<sub>4</sub>-біовугілля до 0.67 мас.ч. CoFe<sub>2</sub>O<sub>4</sub> втрати поглинання композиту сягають –14.15 дБ/мм на частоті 8 ГГц і –12.37 дБ на частоті 12 ГГц.

**Ключові слова:** магнітні властивості; шпінель; рентгенофазовий аналіз.

\*Corresponding author: email: [domosedii@i.ua](mailto:domosedii@i.ua)

© 2025 Oles Honchar Dnipro National University;

doi: 10.15421/jchemtech.v33i4.336256

## Introduction

Cobalt ferrite and composites based on it are of great interest in various fields. They are used as electromagnetic radiation adsorbents, organic synthesis catalysts, photocatalysts, anode materials, magnetic fluid fillers, drug carriers, sensors and information carriers due to their high coercive force at room temperature and intermediate magnetization [1–6]. The wide range of applications of cobalt ferrite is due to the fact that  $\text{CoFe}_2\text{O}_4$  is a mechanically and chemically stable ferrimagnetic material, the cubic structure of which is close to the structure of inverse spinel [7]. Its magnetic properties depend on both the size and shape of the particles and the distribution of ions within the structure [8]. Currently, there are many methods for producing cobalt ferrite and its composite materials – hydrothermal and microwave synthesis, sol-gel, coprecipitation from aqueous and organic media, mechanical grinding and combinations of these methods [9–14]. It is known that materials based on  $\text{CoFe}_2\text{O}_4$  belong to the magnetically controlled variety, which have an important advantage - they can be easily removed from the reaction medium by applying an external magnetic field. This feature expands the scope of application of cobalt ferrite, especially in the case of synthesis of multicomponent composites. For example, graphene, biochar or graphite powder dispersed in an aqueous medium can be removed by its long-term sedimentation, centrifugal separation, etc. This requires a lot of time, energy, complex equipment for use in industrial conditions. Thus, the procedure for extracting nanoscale objects from suspensions is very difficult. Biochar is also often used as a filler for composites. Biochar is an inexpensive, stable, environmentally friendly and sustainable material obtained from available waste biomass by pyrolysis, hydrolysis, gasification and carbonization. Biochar can be used as a base with a developed surface for the deposition of various catalytic nanoparticles due to its unique surface properties, easily tunable functional groups, chemical stability and electrical conductivity. In recent years, various biochar-based materials have been synthesized and described. The described composites demonstrate the capabilities of photocatalysis in the visible part of the spectrum, chemical stability, and the ability to adsorb various pollutants. For example, the properties of the following composites have been described: Mg-Al/biochar composites, Mineral-biochar composites, Layered double hydroxide-biochar composites, Microorganism-biochar

composites [15–17]. The introduction of such compounds into organic matrices such as polyvinyl alcohol combines the properties of inorganic (magnetism, biocompatibility, thermal stability, chemical and corrosion resistance, rigidity, non-toxicity) and organic (elasticity, processability, plasticity, high water permeability, strength) phases and attracts considerable attention for various applications including photocatalysis, adsorption, sensors [18; 19]. The development and use of magnetic polymer composites require targeted optimization of the material composition, as well as verification of specific physicochemical properties. The aim of this work is to synthesize  $\text{CoFe}_2\text{O}_4$ -biochar composites and study their phase composition, structure, photocatalytic properties, absorption of electromagnetic radiation, magnetic properties.

## Experimental

Nanoparticles of cobalt ferrite ( $\text{CoFe}_2\text{O}_4$ ) were synthesized by the hydrothermal method in a high-pressure reactor at a temperature of 200 °C. Biochar was obtained by pyrolysis of wood biomass in an electric mine-type laboratory furnace. The biomass sample was loaded into a cylindrical retort, which was placed in a furnace. After that, the furnace was heated to a temperature of 700 °C. The residue obtained after pyrolysis was stewed dry until completely cooled and then ground.

To study the influence of composition on the properties of cobalt ferrite/biochar composites, samples with different ratios of components were synthesized. The composition of the samples is shown in Table 1.

Table 1

№ sample	Samples composition	
	Composition, wt. part	
	$\text{CoFe}_2\text{O}_4$	biochar
1	1	0
2	0.667	0.333
3	0.333	0.667
4	0	1

PVA/ $\text{CoFe}_2\text{O}_4$ -biochar films were synthesized by solution casting at a ratio of PVA to filler of 1 : 1. The obtained PVA/ $\text{CoFe}_2\text{O}_4$  solutions were cast on flat surfaces and left at room temperature for 48 hours to obtain films (1 mm thick) and remove excess water.

X-ray phase analysis of the samples was carried out on a DRON-2 diffractometer. The operating mode of the X-ray source is 40 kV, 30 mA. The range of scanning angles  $2\theta$  is from 10 to 90°. The morphology and elemental composition of the samples were studied using a JSM-6390LV

scanning electron microscope and an AZtecEnergy X-maxN50 energy-dispersive spectrometer.

Identification and determination of the concentration of methylene blue (MS) was carried out by spectrophotometric analysis using a spectrophotometer UV 5800 PC. To study photocatalysis, a solution of methylene blue with a concentration of 7.6 and 15.2  $\mu\text{mol/l}$  was used.

The absorption and reflection losses of ferrites were measured using a setup consisting of a G4-83 generator, a C4-11 spectrum analyzer, and a biconical resonator. The measurements were performed at a frequency of of  $10^8$ – $10^{12}$  Hz at a temperature of 25 °C.

The magnetic properties of the composites were studied using a vibration magnetometer.

## Results and discussion

### *X-ray diffraction patterns of composites*

Figure 1 shows the X-ray diffraction patterns of polymer composites of different compositions (according to Table 1).

Sample 1 is a cobalt ferrite polymer composite. The X-ray diffraction pattern shows that the composite has characteristic diffraction peaks. The largest of them are marked at  $2\theta$  74.4°, 67.5°, 50.8°, 41.7°, 35.4°, which correspond to the structure of cobalt ferrite. The  $\alpha$ -Fe phase at  $2\theta$  52.7° is also identified in the diffraction patterns. Composites 2 and 3 are characterized by a decrease in all characteristic peaks of cobalt ferrite, which is due to a decrease in its content in the samples. The effect of the biochar content is difficult to assess in the obtained samples, since there are no clearly pronounced peaks, and the X-ray diffraction pattern of composite 4, which includes only pure biochar, reflects its amorphous structure.

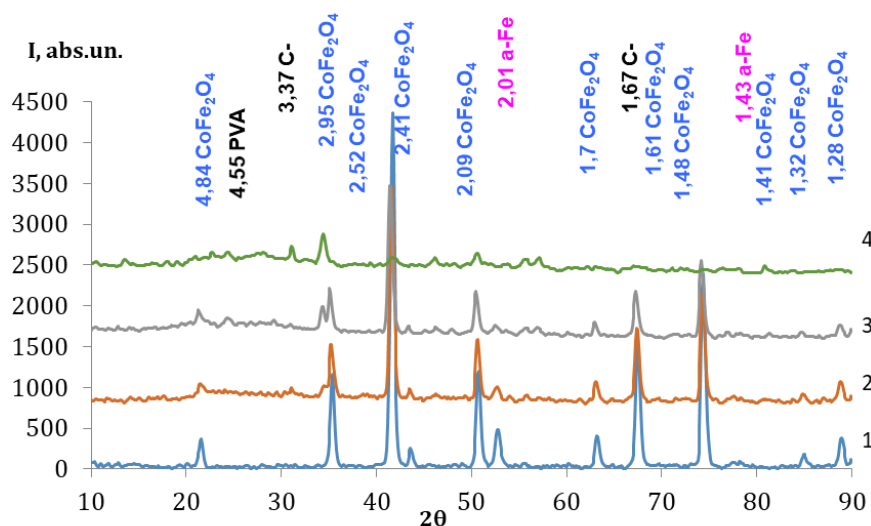


Fig. 1. X-ray diffraction patterns of polymer composites

### *The microstructures of composites*

Figure 2a shows a microphotograph of the biochar, obtained with the help of SEM. It clearly shows a large number of macropores on the surface of wood biochar. These cavities are connected with the structure of the wood of the plant. Cobalt ferrite particles (Fig. 2b), obtained by

the hydrothermal method, have a spherical shape with a diameter of 100-150 nm and are significantly smaller in size than the pores and cavities on the surface of the biochar. This makes it possible to embed ferrite particles and obtain magnetic nanocomposites.

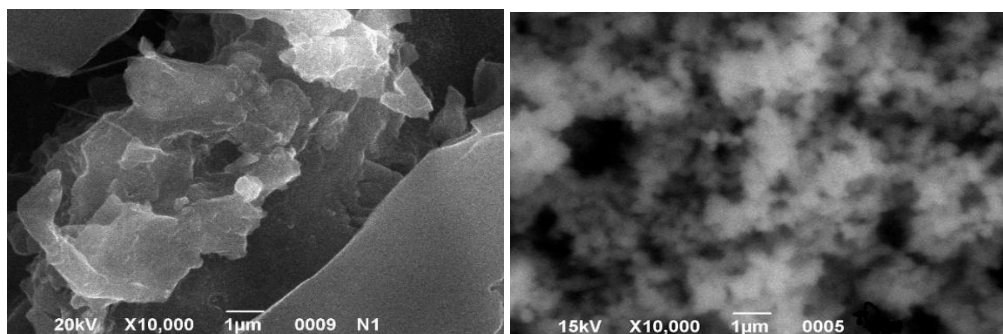


Fig. 2. SEM images of samples a – biochar, b – cobalt ferrite

*Magnetic properties*

Figure 3 shows the magnetic hysteresis loops of PVA/CoFe<sub>2</sub>O<sub>4</sub>-biochar composites.

All samples have a coercive force of 200-370 Oe. The highest values of residual magnetization and saturation magnetization are for sample 1 (45.93 emu/g and 162.87 emu/g, respectively). At the same time, samples 3 and 4 have very low Mr,

Ms, and Hc values, which may indicate that biochar has a negative effect on magnetic properties at the appropriate ratio of components in the composite. Therefore, the concentration of CoFe<sub>2</sub>O<sub>4</sub> has a decisive influence on the parameters of residual and saturation magnetization of composites (Fig. 4). Therefore, by controlling and changing it, the necessary magnetic properties can be achieved.

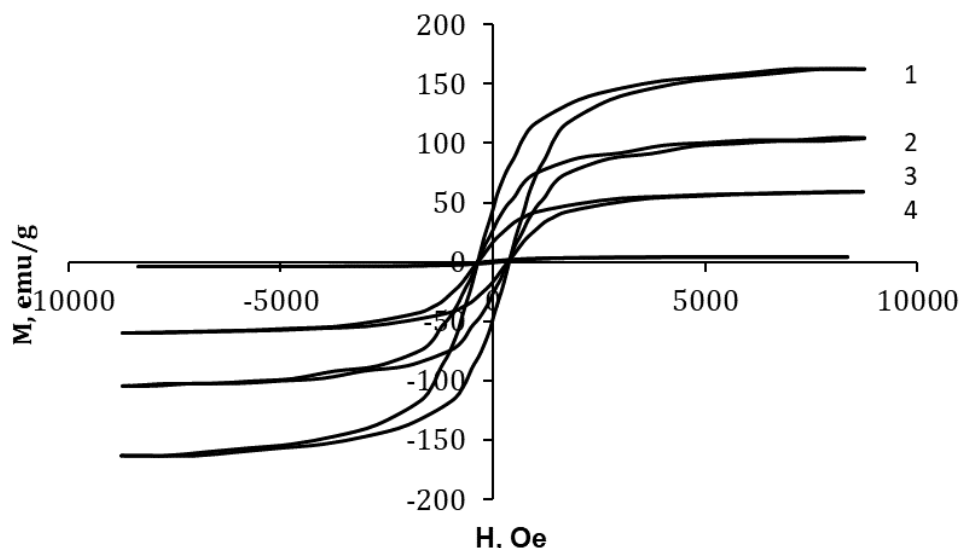


Fig. 3. Magnetic hysteresis loops of samples 1-4

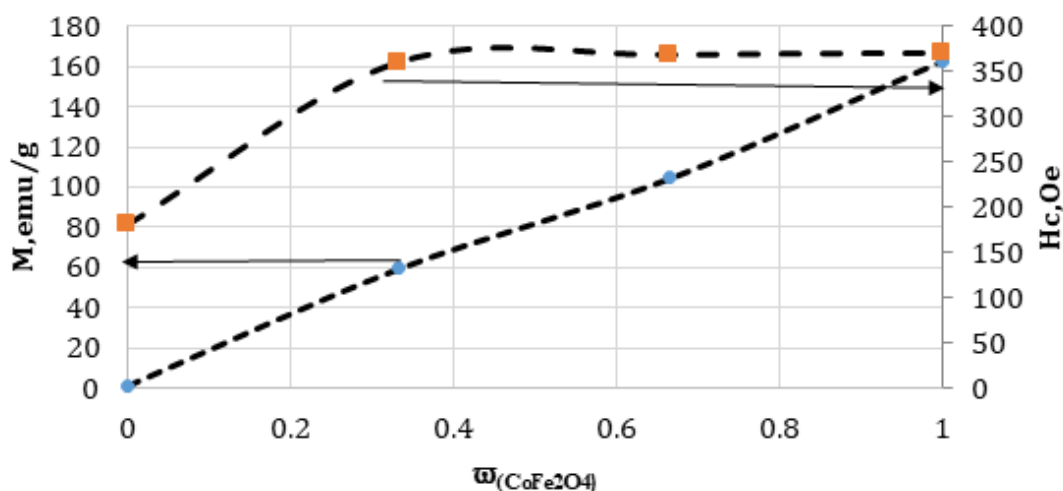


Fig. 4. Dependence of the coercive force and saturation magnetization on the composition of composites

*Photocatalytic ability*

The photocatalytic activity of PVA/CoFe<sub>2</sub>O<sub>4</sub>-biochar composites and PVA/CoFe<sub>2</sub>O<sub>4</sub> and PVA/biochar photocatalysts was evaluated by the degree of degradation of the MB dye under the influence of ultraviolet light. The rate of photodegradation of MB on the obtained PVA/biochar nanocomposite photocatalysts with different contents of biochar and CoFe<sub>2</sub>O<sub>4</sub> under the action of UV is shown in Fig. 5. MB solution was used as the initial solution. It is interesting that CoFe<sub>2</sub>O<sub>4</sub> or biochar are photocatalytically more inert compounds, while the PVA/CoFe<sub>2</sub>O<sub>4</sub>-biochar

composite leads to a sharp increase in photocatalytic activity (Fig. 5). With an increase in the content of biochar in the PVA/CoFe<sub>2</sub>O<sub>4</sub>-biochar photocatalyst, a faster degradation of MB was observed, and 67 % by mass. biochar in the PVA/CoFe<sub>2</sub>O<sub>4</sub>-biochar composite provided the best indicators of photocatalytic activity. It is clearly visible that the degree of destruction of MB in the solution was 98 % after 60 min. Studies have shown that similar patterns are observed for initial concentrations of MB of 7.6 and 15.2  $\mu\text{mol/l}$ .

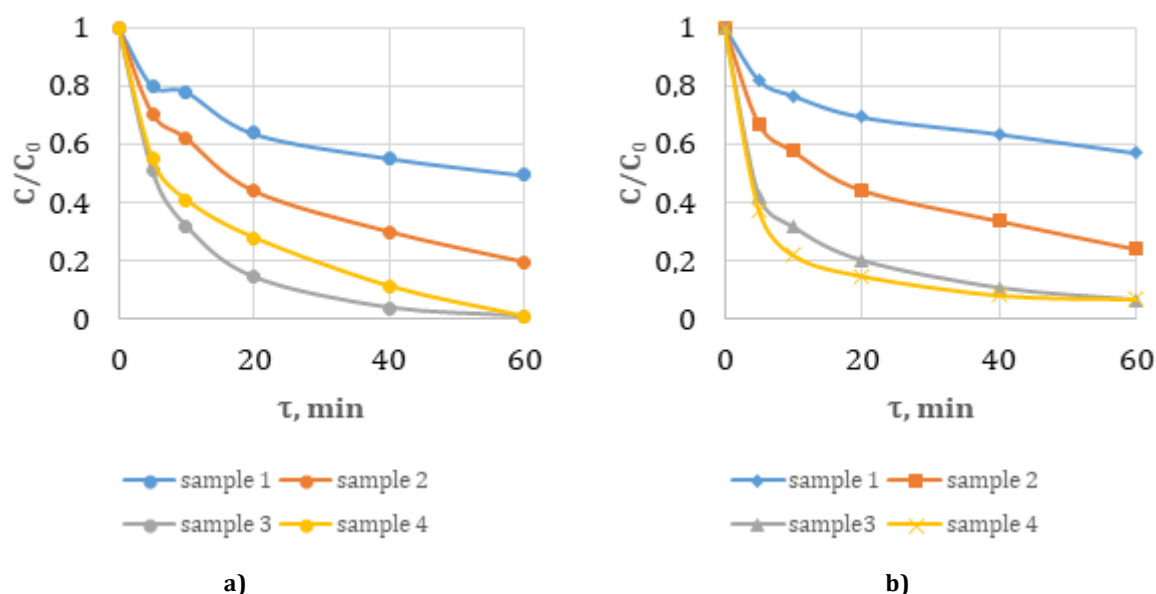


Fig. 5. Photocatalytic destruction of methylene blue (a-concentration 7.6 μmol/l, b-15.2 μmol/l)

The calculated decomposition rates for MS are summarized in the diagrams (Fig. 8 (a, b) concentrations of 7.6 μmol/l and 15.2 μmol/l of respectively).

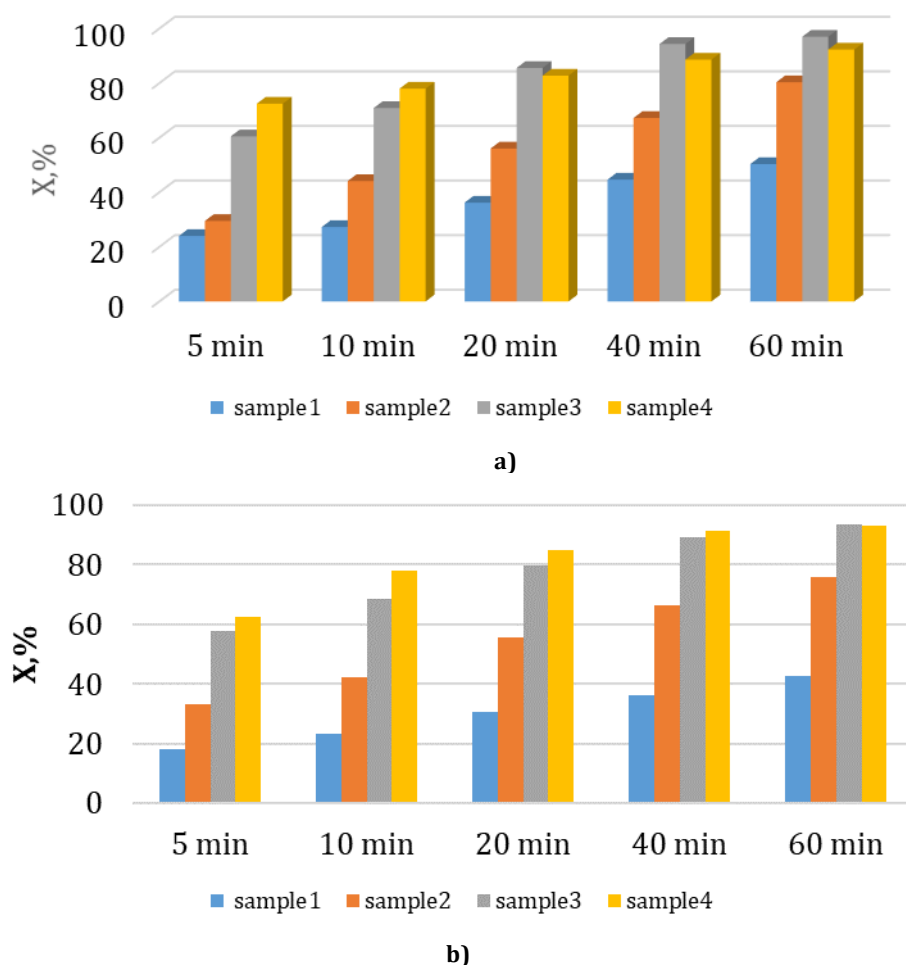


Fig. 8. Histogram of the degree of decomposition of methylene blue (a – concentration 7.6 μmol/l; B – 15.2 μmol/l)

The diagrams show that at a lower concentration of MB in the solution, the best was sample 3 with approximately 97 % purification

degree in 60 min. An increase of two times of the initial concentration of MB shows a similar pattern: samples 3 and 4 are the most effective, the

degree of destruction is 93% and 93.4%, respectively.

Calculations showed that the reaction of photocatalytic decomposition of MB obeys pseudo-first-order kinetics.

Kinetic data on the decomposition of MB are described by the first-order rate equation:

$$-\ln\left(\frac{C_t}{C_0}\right) = Kt$$

where K is the reaction rate constant,

$C_0$  and  $C_t$  are the initial MB concentration and the concentration at the irradiation time t, respectively.

Table 3 shows the values of the pseudo-first-order rate constant and the correlation coefficient for photodegradation of MB by photocatalysts of PVA/CoFe<sub>2</sub>O<sub>4</sub>-biochar composites with different biochar content at different initial MB concentrations. Among these catalysts, biochar showed the highest rate constant of 0.085 min<sup>-1</sup>, PVA/CoFe<sub>2</sub>O<sub>4</sub>-biochar composites – 0.05 min<sup>-1</sup>. On the contrary, the PVA/CoFe<sub>2</sub>O<sub>4</sub>-biochar composite with a lower biochar content showed a lower rate

constant, and the photocatalytic activity of pure CoFe<sub>2</sub>O<sub>4</sub> was quite low.

Table 3

Kinetic parameters of MB decomposition				
Sample number	Rate constant, min <sup>-1</sup>	R <sup>2</sup>	Rate constant, min <sup>-1</sup>	R <sup>2</sup>
	MB concentration 7.6 μmol/l,		MB concentration 15,2 μmol/l	
1	0.014	0.89	0.012	0,98
2	0.028	0.95	0,027	0,99
3	0.050	0.96	0,048	0,98
4	0.085	0.99	0.061	0.99

#### Microwave adsorbing properties of composites

Fig. 9 shows the absorption characteristics of various PVA/CoFe<sub>2</sub>O<sub>4</sub>-biochar composites in the radar range from 8 GHz to 12 GHz. It can be seen that the content of ferrite has an obvious effect on the absorption properties of microwave radiation. Polymer composite 2 reaches a maximum absorption value of -14.15 dB, in the range from 8 GHz to 12 GHz. Moreover, significant absorption losses are observed in the entire measured range.

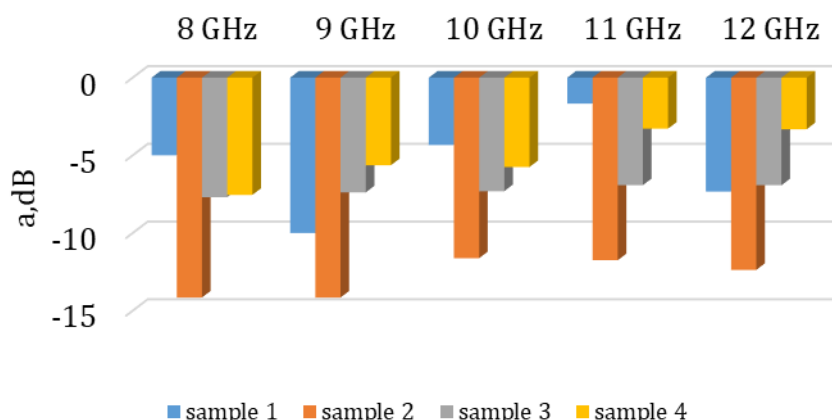


Fig. 9. Absorption characteristics of various composites in the range of 8–12 GHz

#### Conclusions

The magnetic material CoFe<sub>2</sub>O<sub>4</sub>-biochar with different biochar contents was successfully prepared by a two-stage combined method. The results of electron microscopy show that biochar has a block structure with large pores, so this structure can be used in the creation of composites. Measurements of photocatalytic activity show that the combination of CoFe<sub>2</sub>O<sub>4</sub> nanoparticles with biochar blocks leads to a sharp transformation of the less active cobalt ferrite into a highly active catalyst for the decomposition of

MB under the action of UV light. A significant increase in photocatalytic activity can be ensured by the presence of biochar.

When studying the absorption of electromagnetic radiation in the radar range from 8 GHz to 12 GHz of PVA/CoFe<sub>2</sub>O<sub>4</sub>-biochar composites, it can be seen that the polymer composite with a CoFe<sub>2</sub>O<sub>4</sub> content of 0.667 mol. parts reach an average absorption value of about 12.5 dB, in the range from 8 GHz to 12 GHz. The content of cobalt ferrite in the composite is decisive.

#### References

- [1] Xuan, C. T. A., Tho, P. T., Xuan, N. D., Ho, T. A., Ha, P. T. V., Trang, L. T. Q., Tran, N. (2024). Microwave absorption properties for composites of CoFe<sub>2</sub>O<sub>4</sub>/carbonaceous-based materials: A comprehensive review. *Journal of Alloys and Compounds*, 990, 174429. <https://doi.org/10.1016/j.jallcom.2024.174429>
- [2] Xu, K., Zhu, Z., Hu, C., Zheng, J., Peng, H., Liu, B. (2024). Superior degradation of organic contaminants by the



- UV/CoFe<sub>2</sub>O<sub>4</sub>/PI system: Kinetics, pathways, mechanisms and DFT calculation. *Separation and Purification Technology*, 336, 126197. <https://doi.org/10.1016/j.seppur.2023.126197>
- [3] Zhang, Y., Guo, J., Ji, Z., Hou, J. (2024). Synthesis and photocatalytic application of magnetic CoFe<sub>2</sub>O<sub>4</sub>/conjugated poly (vinyl chloride) derivative nanocomposite. *Langmuir*, 40(31), 16642–16652. <https://doi.org/10.1021/acs.langmuir.4c02349>
- [4] Wang, F., Zhang, Y., Peng, Y., Xiao, W., Yu, W., Wang, H., Bian, Z. (2024). Continuous peroxymonosulfate activation for antibiotics degradation via fluorine-free-Ti<sub>3</sub>C<sub>2</sub>Tx-CoFe<sub>2</sub>O<sub>4</sub> hydrogel beads: Performance, mechanism and application. *Applied Catalysis B: Environment and Energy*, 358, 124441. <https://doi.org/10.1016/j.apcatb.2024.124441>
- [5] Abbas, M. H., Ibrahim, H., Hashim, A., Hadi, A. (2024). Fabrication and tailoring structural, optical, and dielectric properties of PS/CoFe<sub>2</sub>O<sub>4</sub> nanocomposites films for nanoelectronics and optics applications. *Transactions on Electrical and Electronic Materials*, 25(4), 449–457. <https://doi.org/10.1007/s42341-024-00524-5>
- [6] Hussein, M. M., Saafan, S. A., Abosheisha, H. F., Zhou, D., Tishkevich, D. I., Abmiotka, N. V., Darwish, M. A. (2024). Preparation, structural, magnetic, and AC electrical properties of synthesized CoFe<sub>2</sub>O<sub>4</sub> nanoparticles and its PVDF composites. *Materials Chemistry and Physics*, 317, 129041. <https://doi.org/10.1016/j.matchemphys.2024.129041>
- [7] Hou, Y. H., Zhao, Y. J., Liu, Z. W., Yu, H. Y., Zhong, X. C., Qiu, W. Q., Wen, L. S. (2010). Structural, electronic and magnetic properties of partially inverse spinel CoFe<sub>2</sub>O<sub>4</sub>: a first-principles study. *Journal of Physics D: Applied Physics*, 43(44), 445003. doi 10.1088/0022-3727/43/44/445003
- [8] Senthil, V. P., Gajendiran, J., Raj, S. G., Shanmugavel, T., Kumar, G. R., Reddy, C. P. (2018). Study of structural and magnetic properties of cobalt ferrite (CoFe<sub>2</sub>O<sub>4</sub>) nanostructures. *Chemical Physics Letters*, 695, 19–23. <https://doi.org/10.1016/j.cplett.2018.01.057>
- [9] Arora, K., Ledwani, L., Komal. (2025). A Comprehensive Review on the Synthesis and Therapeutic Potential of Cobalt Ferrite (CoFe<sub>2</sub>O<sub>4</sub>) Nanoparticles. *Chemistry Select*, 10(1), e202404136.
- [10] Frolova, L. A., Sknar, I. V. (2024). Study of the influence of synthesis parameters on the structural and magnetic properties of cobalt ferrite. *Journal of Chemistry & Technologies*, 32(1). <https://doi.org/10.1002/slct.202404136>
- [11] Frolova, L. (2020). Photocatalytic activity of spinel ferrites Co<sub>x</sub>Fe<sub>3-x</sub>O<sub>4</sub> (0.25 < x < 1) obtained by treatment contact low-temperature non-equilibrium plasma. *Applied Nanoscience*, 10(12), 4585–4590. <https://doi.org/10.1007/s13204-020-01344-8>
- [12] Liandi, A. R., Al-wahid, A. A., Siregar, Y. D. I., Wendari, T. P., Cahyana, A. H., Insani, A. (2024). Green mussel shell-derived hydroxyapatite-CoFe<sub>2</sub>O<sub>4</sub> catalyst: Microwave-assisted synthesis of 2-amino-4H-chromene derivative. *Case Studies in Chemical and Environmental Engineering*, 10, 100851. <https://doi.org/10.1016/j.cscee.2024.100851>
- [13] Mohan, H., Mohandoss, S., Prakash, A., Balasubramanian, N., Loganathan, S., Assadi, A. A., Khacef, A. (2024). Cold plasma assisted synthesis of spinel-CoFe<sub>2</sub>O<sub>4</sub> nanoparticle with narrow bandgap and high magnetic activity. *Inorganic Chemistry Communications*, 167, 112754. <https://doi.org/10.1016/j.inoche.2024.112754>
- [14] Hussein, H., Ibrahim, S. S., Khairy, S. A. (2025). Sustainable synthesis of CoFe<sub>2</sub>O<sub>4</sub> nanoparticles with tailored physical properties using Hibiscus extract for photo-Fenton catalytic degradation of methylene blue dye: Response surface methodology. *Journal of Water Process Engineering*, 76, 107893. <https://doi.org/10.1016/j.jwpe.2025.107893>
- [15] Pan, X., Gu, Z., Chen, W., Li, Q. (2021). Preparation of biochar and biochar composites and their application in a Fenton-like process for wastewater decontamination: A review. *Science of the Total Environment*, 754, 142104. <https://doi.org/10.1016/j.scitotenv.2020.142104>
- [16] Liang, L., Xi, F., Tan, W., Meng, X., Hu, B., Wang, X. (2021). Review of organic and inorganic pollutants removal by biochar and biochar-based composites. *Biochar*, 3(3), 255–281. <https://doi.org/10.1007/s42773-021-00101-6>
- [17] Wang, L., Ok, Y. S., Tsang, D. C., Alessi, D. S., Rinklebe, J., Mašek, O., Hou, D. (2022). Biochar composites: Emerging trends, field successes and sustainability implications. *Soil Use and Management*, 38(1), 14–38. <https://doi.org/10.1111/sum.12731>
- [18] Frolova, L. A., Pasenko, O. O., Sukhyi, K. M. (2022). Характеристика композитного полімерного матеріалу діатоміт-альгінат-Fe<sub>3</sub>O<sub>4</sub>. *Journal of Chemistry and Technologies*, 30(2), 229–239. <https://doi.org/10.15421/jchemtech.v30i2.243768>
- [19] Mahmoud, M. E., Abouelanwar, M. E., Mahmoud, S. E. M., Salam, M. A. (2022). Adsorption behavior of silver quantum dots by a novel super magnetic CoFe<sub>2</sub>O<sub>4</sub>-biochar-polymeric nanocomposite. *Journal of Colloid and Interface Science*, 606, 1597–1608. <https://doi.org/10.1016/j.jcis.2021.08.102>